CHONK 1.0: landscape evolution framework: cellular automata meets graph theory

Boris Gailleton[1,2], Luca Malatesta[1], Guillaume Cordonnier[3], and Jean Braun[1]

[1]CNRS, Géosciences Rennes, University of Rennes, Rennes, France
[2]Earth Surface Process Modelling, GFZ German Research Center for Geosciences, Potsdam, Germany
[3]Université Côte d'Azur and INRIA, Sophia-Antipolis, France

Correspondence: Boris Gailleton (boris.gailleton@univ-rennes1.fr)

Abstract. Landscape Evolution Models (LEMs) are prime tools to simulate the evolution of source-to-sink systems through ranges of spatial and temporal scales. Plethora of different empirical laws have been successfully applied to describe the different parts of these systems: fluvial erosion, sediment transport and deposition, hillslope diffusion, or hydrology. Numerical frameworks exist to facilitate the combination of different subsets of laws, mostly by superposing grids of fluxes calculated

5   independently. However the exercise becomes increasingly challenging when the different laws are inter-connected: for example when a lake breaks the upstream-downstream continuum of the amount of sediment and water it receives and transmits; or when erosional efficiency depends of the composition of a sediment flux affected by multiple processes. In this contribution, we present a method mixing the advantages of cellular-automata and graph theory to address such cases. We demonstrate how the former guarantees finite knowledge of all fluxes independently from the process-law implemented in the model while

10   the latter offer a wide range of tools to process numerical landscapes, including landscapes with closed basins. We provide three scenario largely benefiting from our method: i) one where lake systems are primary controls on Landscape evolution, ii) one where sediment provenance is closely monitored through the stratigraphy and iii) one where heterogeneous provenance influences fluvial incision dynamically. We finally outline the way forward to make this method more generic and flexible.

1 Introduction

15   The lifespan of a sediment - from erosion upstream, transport, and then deposition downstream - and the accompanying impact to the evolution of the landscape are relatively short compared to the usual time-scales of other geological processes. However, its large spatial footprint on areas with little accessibility and the interleaving of sediments with other processes makes them difficult to measure and observe directly (e.g. Sadler, 1981; Jerolmack and Sadler, 2007; Ganti et al., 2011; Schumer et al., 2017). Various models, from analogue (experimental) to numerical, are natural tools to explore the source-to-sink system at

20   different time and spatial scales. Analogue models offer a time compression in scaled experiments to simulate rapidly long timespans with complex physics but relatively simple environmental forcing (Babault et al., 2005; Paola et al., 2009; Guerit et al., 2014). Alternatively, numerical Landscape Evolution Models (LEMs) have the advantage of giving complete control of the simulation. However they rely on mostly empirical laws and are often limited to specific geoscience problems. For example, the evolution of surface topography over millions of years can be efficiently explored with erosion laws that largely simplify -

I do not understand. These LEMs do not ignore sediment transport at all.

25 or completely ignore - sediment transport (e.g. Braun and Willett, 2013; Yuan et al., 2019; Hergarten, 2020). On the contrary, bedrock incision can be advantageously ignored when the focus is a high resolution modeling of sediment redistribution at very short time-scales (e.g., Sklar and Dietrich, 1998; Croissant et al., 2017; Coulthard et al., 2013; Roelvink and Van Banning, 1995, or). A major challenge therefore lies in finding the right combination of laws to best address a given problem (Barnhart et al., 2019). That is complicated by the significant impacts of any change in numerical or physical parameters both in terms of

30 quantitative results and computation time (e.g. Campforts et al., 2017; Armitage, 2019; Grieve et al., 2016).

While some process laws are implemented in standalone models (e.g. Hergarten, 2020; Braun and Sambridge, 1997; Coulthard et al., 2013), mature frameworks exist to facilitate the combination of different LEMs components and exploring their results (e.g. Barnhart et al., 2020; Bovy, 2019; Schwanghart and Scherler, 2014; Mudd et al., 2019). However, these frameworks and models are designed to combine process-laws at grid level where for example, minima, flow routing or

35 river incisions are successively and independently solved. This can be a problem when studying more complex source-to-sink systems with multiple processes that are inter-connected. One could imagine a situation where an intermediate lake acts as a local sink, and its filling depends on any process involving sediments or water upstream (Figure 1). Its filling will, in turn, impact the behaviour of the process law downstream depending on the amount of water and sediments they can or cannot transmit. This is incompatible with grids solved independently, or requires exchange data structures that would increase the

40 run-time exponentially. Beyond the question of local minimas, the role of sediment fluxes is perhaps the most representative example of inter-connectivity. It is recognized as a potential important factor in the dynamics of catchment evolution and the record of tectonic and climatic information across timescales (Figure 1). Its implementation in LEM is a logical consequence. Sediment starving or an abundance of clasts in a river will impede bedrock erosion by a lack of tool or an excess cover (Sklar and Dietrich, 2004; Finnegan et al., 2007; Geurts et al., 2018). The relative strengths of erosive clasts and erodi-

45 ble bedrock can also significantly enhance or diminish the erosion efficiency of a river and trigger local (e.g. Gailleton et al., 2021) and non-local consequences (Sklar and Dietrich, 2001). Alluvial dynamics matter also evidently in source-to-sink studies: aggradation-incision cycles in mountain piedmonts can delay sediment delivery to the ocean by > 10 kyr, a climatically relevant timescale, and recycle old signals in the sediment stream (e.g., Clift and Giosan, 2014; Malatesta et al., 2018; Dingle et al., 2020). Modulation of sediment fluxes also lead to prominent alluvial terraces and surfaces that are key for landscape

50 interpretation (Bufe et al., 2017; Tofelde et al., 2017; Malatesta and Avouac, 2018). Increasingly fine resolution in stratigraphic studies warrant a renewed attention to the trajectory of sediment tracers across the landscape (Tofelde et al., 2021). New methods allow the exploitation of new sedimentary signatures requiring a precise understanding of the rate and path of transport of sediment across landscapes (e.g., Lupker et al., 2017). Modelling sediment fluxes at the level of details that field and analytical studies now attain requires a holistic approach rather than the independent implementation of individual processes.

55 In this contribution, we propose a novel methodology, CHONK, to develop frameworks that include fine-grained modularity in a cell-based referential from the ground up, to ensure inter-connectivity between LEMs properties. CHONK is built to guarantee unconditional access to a common numerical toolkit regardless of the type of geomorphological laws employed. The cell-based referential allows the tracking of parameters and/or the exploration of dynamic feedback within the different fluxes transported from a cell to another. We demonstrate the potential of integrating cellular automata elements with graph-based

60 finite difference methods to resolve sedimentary dynamics necessary for sedimentological studies of landscape evolution. This contribution deals with the core architecture of CHONK, while several collaborative projects employ and apply the framework to address sedimentological and geomorphological challenges. These projects concurrently inform the development of a user-friendly platform to be progressively released in the coming months and years.

First, we concisely present and motivate the new method. We then detail the model structure, its different algorithms, and the
65 process laws we picked for the demonstration. Finally, we present and discuss different scenarios demonstrating the capabilities of this new method.
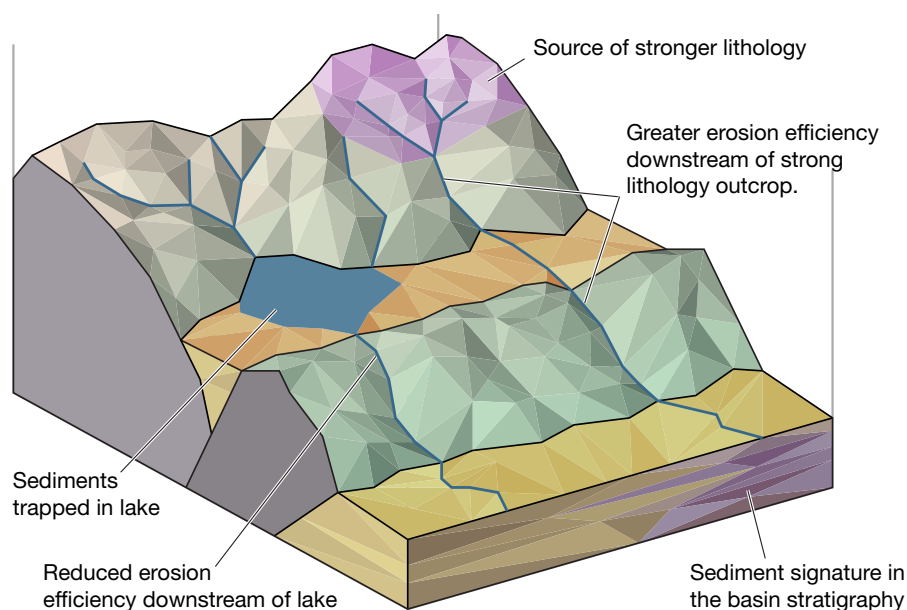

Figure 1. Cartoon landscape highlighting several key attributes of the sedimentary system that CHONK is designed to solve with a novel approach blending cellular automata and graph-based methods. The different domains, connected by the river network and hillslopes transfers of material highlight the interconnected nature of the different processes.

2   Background and motivations

The new formulation we introduce in this contribution is mixing the advantages offered by the cellular automata methods (von Neumann, 1951; Wolfram, 1984) and graph-based finite difference methods commonly used in landscape evolution models and
70 frameworks (e.g. Bovy, 2019; Barnhart et al., 2020; Garcia-Castellanos and Jiménez-Munt, 2015; Braun and Willett, 2013). We first briefly define and review the existing methods and framework to explain our motivations creating a new one.
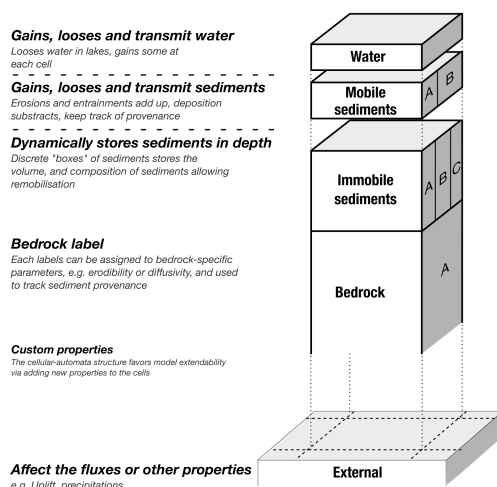
Figure 2. Cartoon illustrating the cellular automata data-structure put in place in this model, with the explanation of the cell structure. These cells are then plugged onto a graph, taking advantage of classic LEM algorithm to process the cell in the right topological order.

2.1 LEM frameworks and methods

LEM frameworks typically independently solve the different components of landscapes evolution modelling following a graph-based logic applied on data grids. In other words, fluxes and other quantities (e.g. elevation, erosion, water) are discretised on 2D arrays that are calculated and combined successively. This can be illustrated with the stream-power incision model (HOWARD and KERBY, 1983). Fluvial incision is defined as a function of slope and drainage area, and the model calculates each component separately for the whole landscape. Grids holding the values of drainage area accumulated from a graph structure and topographic slope are first independently calculated from a topographic 2D array. Both data grids are then combined with an erodibility parameter to calculate fluvial incision rates in each cell. Such grid-based formulation is very flexible and makes the addition or modifications to adapt the model to a geoscientific problem (e.g. adding hillslope diffusion) or an alternative methods (e.g. steepest descent or multiple flow direction calculation of drainage area) straightforward. However, combining independently calculated grids reaches its limitations when processes are interdependent (e.g. the explicit filling of a lake depends on all upstream input and affects every downstream ones which cannot be calculated independently in a unique time step). Simulating dynamic feedbacks remains possible (e.g. Garcia-Castellanos and Jiménez-Munt, 2015; Cordonnier et al., 2018; Salles, 2019), but it requires significant work redesigning processes to statically encompass all the wanted features, or to bypass problematic processes. There is an unavoidable loss of flexibility and modularity when the processes are statically bound to a specific implementation.

2.2 Cellular automata method

Cellular automata models are reduced complexity models designed to tackle discretised problems on networks of connected
90 cells (von Neumann, 1951; Wolfram, 1984). The cells have given properties and states which evolve as a function of the
states of their neighbours according to a set of rules. Road traffic modelling by Nagel and Schreckenberg (1992) is a good
illustration of cellular automata logic. Cells represent a stretch of road and their properties includes, for example, the presence
or absence of cars, their velocity, or whether they are Honda Jazz. Cells evolve as a function of the presence of cars in their
linked counterparts following simple rules to simulate road traffic. Cellular automata methods are not restrained to reduced
95 complexity models, and can include more sophisticated equations and processes. It has been utilised for modelling elements
of landscapes evolution element like water and sediment fluxes (Coulthard et al., 2013); tracking particles in flow (e.g Tucker
et al., 2016); hillslope evolution (e.g. Tucker and Bradley, 2010; Jyotsna and Haff, 1997); soil erosion (e.g. D'Ambrosio et al.,
2001); sediment transport and channel morphology (e.g. Salles et al., 2007). Frameworks exist to take advantage of cellular
automata (e.g. Tucker et al., 2016, , partially implemented in Barnhart et al. (2020)). One limitation of a purely cellular automata
100 model is that cells are processed at the same time at each time step, which is not compatible with quantities that are informed
by spatial integration like the downstream accumulation of drainage area or sediment flux.

2.3 Hybrid solution: cellular automata on a graph

Above I only see one method, the cellular automata one. The graph method has not been presented yet

We developed a new formulation combining the <mark>two methods outlined above.</mark> We process a topographic grid from which we
calculate a graph of downstream/upstream connectivity, but every nodes on the grid is treated as a cell. The properties of the
105 cells are the quantities and fluxes the set of equation implemented in the model needs - e.g. elevation, bedrock incision, water,
sediment fluxes (Figure 2). Like cellular automata methods, all the calculations modifying fluxes and quantities are processed
in the cell referential, i.e. all processes within a single cells are processed before transmitting fluxes to neighbouring cells.
However like long-term grid-based LEMs, the cells are processed in a specific order following a topology dictated by the
topographic graph. In other words, when a cell is processed, all its upstream counterparts are already fully processed and the
110 final state of all upstream fluxes can be known. With this formulation, only the interactions from a cell to its neighbours (or
some of its neighbours) needs to be defined. In this contribution, we aim to demonstrate that this method is particularly adapted
to solve problems and challenges involving interdependent feedback that are difficult to tackle otherwise.

Local minima are integrated into the structure of the model and allow lakes and endhoreic basins to be treated as separated
domains while keeping a concept of upstream-downstream with the rest of the landscapes. This hybrid solution s also ensures
115 inter-connectivity between and within the cells. This crucial feature allows (i) tracing the state of any properties at any point
(e.g. provenance, residence time, ...) and (ii) using this inter-connectivity directly in process laws (e.g. using the composition
of the sediment flux to influence river incision). Finally, the hybrid solution simplify the numerical implementation of laws
which needs to only be expressed function of one generic cells and its neighbours.

120   The prototype we developed for this contribution is a first step toward a fully-fledged, generic and dedicated framework like
Barnhart et al. (2020). We implemented a specific set of process-law in order to test and demonstrate the advantages of this
method.   Here I still do not understand the difference in philosophie with previous LEMs

2.4   Comparison with existing models or frameworks

A number of numerical tools already exist for Landscape Evolution Modelling. It is not in the scope of this manuscript to
provide an exhaustive review of all of them as them, but it is important to mention the ones most relevant to our goals.

125   Cellular automata models have been utilised for landscapes evolution models at basin scale. Coulthard et al. (2013) devel-
oped CAESAR-LISFLOOD, a cellular automaton model approximating the shallow-water equations (Bates et al., 2010) and
designed to explore fluvial sediment transport and bedrock erosion over the timescale of few thousands of years. Like other
landscape evolution models solving similar equations (e.g. Davy et al., 2017; Adams et al., 2017), this family of methods is not
designed for geological and/or mountain-range scale because they are (i) numerically limited by the short time steps required

130   to keep the finite difference scheme stable and (ii) philosophically limited by the amount of external constraints required (high
resolution precipitation patterns for example). CAESAR-LISFLOOD also processes all the cells in any arbitrary order (or even
in parallel), rather than a systematic downstream succession as it does not need to accumulate downstream a variable within a
single time step.   Not entirely true. CASESAR has a specific algorithm but aiming at calculating the field of accumulated
water discharge in order to solve the sediment transport field by taking into account the downstream
propagation of sediment

The landscape evolution modelling community relies on well-established frameworks helping the development and the

135   design of landscape evolution models, or more generally of topographic data (Barnhart et al., 2020; Schwanghart and Kuhn,
2010; Mudd et al., 2019; Bovy, 2019). Our method has overlaps with their principle, as both process topographic data as
primary input. They all rely on routines manipulating a topographic grid and building a graph of node connectivity for it.
However, existing frameworks are primarily designed to be solved on grids alone and inherit their limitations (section 2.1).

Taking explicit account of lakes is one of the main feature of our method but different approaches already exist. A common

140   family of methods consists in preprocessing the local minima by altering the topography in order to force them to drain by
either carving a way to an output (Lindsay, 2016) or filling them (Wang and Liu, 2006; Barnes et al., 2014a). Both force the
local minima to connect to the rest of the landscapes, and to escape it via the edges. Bovy (2019) utilises an alternative method
by Cordonnier et al. (2018) leveraging graph theory to simulate carving/filling without affecting topography. It is worth noting
that some algorithms have been specifically develop to explicitly process, calculate and fill depressions with arbitrarily given

145   amount of water (e.g. L. Callaghan and D. Wickert, 2019; Barnes et al., 2019, 2021). However, these methods are only designed
to fill pits with water and would require significant amount of modifications to be utilised as cellular automata processor, or even
to any other purpose than what they are designed for. Some landscape evolution models or studies allow the explicit accounting
of lakes. Geurts et al. (2018) for example utilised Braun and Sambridge (1997) to simulate lake filling by stopping flow at lake
bottom and only connecting the lake to the rest of the landscapes once filled with fluvial sediments. Campforts et al. (2020) or

150   Yuan et al. (2019) enhanced fluvial deposition in lake areas in order to roughly approximate lake deposition. These methods
acknowledge the importance of lakes in the landscapes, but do not fully embrace them as separate entities. Salles (2019)
characterise lakes, by first filling the topography with Barnes et al. (2014a) and identifying areas the topography changes.

After a first reading I think I understand
what you mean but this was not the case
at the first reading.

6

Their model then traps all the sediment carried in these domains, transmitting potential excess to the downstream landscape. This method is close to what we aim to achieve but considers lake as unconditionally filled and outletting, thus not designed for

155   endhoreic basins. TISC (formerly described in Garcia-Castellanos and Jiménez-Munt, 2015) is a pioneer in term of integrating endorheism to LEMs and recognising its impact on landscape evolution (Garcia-Castellanos et al., 2003; Garcia-Castellanos, 2006; Struth et al., 2021). TISC calculates the topography of the depressions and fill them gradually with the available sediment and water. Excess material is only transmitted to the outlet and downstream landscapes if available, successfully simulating closed lake and endorheism when lake evaporation or infiltration balances precipitation. Their implementation however differs

160   from our contribution in term of design: water fluxes are calculated separately from the rest of the processes. Runoff is first calculated and the lakes are gradually filled, dynamically accounting for evaporation and lake spilling. Other processes are only calculated after the water flux is defined whereas where CHONK calculates all the fluxes simultaneously for each separated cells, allowing inter-connectivity between the properties.

Finally, tracking sediment provenance in landscape evolution models has been done before in different ways. Carretier et al.

165   (2016) add discrete Lagrangian particles on top of Eulerian grids. They post-process erosion, entrainment and deposition of sediment fluxes to determine the movement of these particles with a probabilistic approach. Sharman et al. (2019) integrate the erosion field to back calculate provenance from labeled areas. These existing methods have in common that they are post-processing the tracking, i.e. calculating the proportion of sediment provenance after the calculation of the surface process laws. We aim in this contribution to embed the trackers into the model in order to make possible their integration directly in the

170   process laws, for example adjusting fluvial erosivity to the proportion of a certain rock type it contains relative to the rock type it bounces on.

3   Model implementation

3.1   Building a directed acyclic graph

The first step consists in building a graph of connectivity in our landscape in order to determine a lake-aware notion of upstream

175   and downstream. This represents the "rail" on which the cells are being processed in order. We use a regular rectangular grid to discretised topographic elevation, noted z. Each individual node of the matrix becomes a cell, noted i. Each cell is connected to adjacent neighbours with the D8 direction, i.e. encompassing all the cells in diagonals and side directions. This defines the node graph, where for any given cell i we call its receivers r_i all the connected cells with lower z and its donors d_i all the connected cells with higher z. Cells with no donors are referred as source cells while cells with no receivers are pits (if internal) or edges

180   (if located on a matrix boundary). We implemented two types of boundary conditions defining neighbouring at the edges: (i) open boundaries, where fluxes can escape the model and the cell has no receivers, and (ii) periodic boundaries, where the fluxes communicate with the opposite cells (*e.g* a cell at the eastern boundary is linked to its opposite at the western boundary). The graph hence created is a Directed Acyclic Graph (DAG): each cell is linked to one or several receivers and cannot cycle back to itself. In graph theory, setting up a DAG allow for the use of a wide range of dedicated algorithms for topological ordering or

format citation

185 graph traversals. The type of flow emulated by this DAG is called a Multiple Flow Direction Schwanghart and Scherler (2014) as one cell can be linked to multiple receivers.

Note that the case of numerically flat surfaces, i.e. a node surrounded by others with the exact same elevation at numerical precision, needs particular care. In such situations, neighbours of i can end up being neither a receiver nor a donor and can gen-190 erate cycles. Methods exist to process the flat surfaces (e.g, Barnes et al., 2014a). We use the carving algorithm by Cordonnier et al. (2018) to approximate an acyclic flow direction on these flat surfaces, the algorithm is detailed in the next subsection.

3.2 Computing a depression-aware topological order

give an example

Once the connection between cells is established, we compute the topological order. It is a crucial step for any landscape evolution model: it determines the order at which cells need to be processed to start from the source nodes and finish with the edges. Alternative methods exist: it is possible, for example, to utilise an iterative method accumulating fluxes progressively 195 (e.g. Braun and Sambridge, 1997); solving large sparse matrices (e.g. Perron, 2011); using priority queue data structures to traverse dynamically the graph of cells (e.g. Barnes et al., 2014b, 2019). Computing a topological order allows us to process cells one by one as requested by our model design.

As in all LEMs with an explicit numerical schema (e.g. CIDRE). I miss something.

What is it ?

Our implementation of an algorithm calculating a depression-aware topological order needs therefore to satisfy a number of conditions: (i) conservation of the original topography of the depression in order to explicitly take account of its characteristics 200 and (ii) respect the notion of upstream and downstream accounting for potentially local minima systems. We implemented two

Do you mean lakes ?

different algorithms to incorporate local minimas in the model. First, a topological order implicitly taking account of local minimas approximating flow path as if depressions were recognized but assumed to be entirely filled up to the elevation of the outlet . And second, an algorithm designed to explicitly accounting for the potential volume of lakes, effectively handling them separately, potentially closed domains with dedicated processes. Both of the algorithms modify the DAG in order to emulate 205 a notion of upstream/downstream by linking the pit nodes of the different depressions to an adequate outlet node. Finally an algorithm takes advantage of the modified DAG to calculate the depression-aware topological order.

We use the same algorithm to calculate the topological order for both implicit and explicit scena   The algorithm is a modified implementation of the one in fastscape (Bovy, 2019, Braun J., pers. com.) and very similar than the one described in Anand et al. (2020). It is $O(n)$ in complexity with n being the total number of links between the cells and their receivers in 210 the graph. In short, a queue is initialised with the source cells. In turn, these are popped out of the queue, pushed into a stack array and their receivers are visited. An array tracks the number of times each cell is visited. If the number of visits equals the number of donors of a given node, it is saved into the stack and process in turns. Once the queue emptied, all the cell have come through and the stack array contains all the node indices ordered. This stack array can be traversed in normal or reverse order to respectively process upstream or downstream cells first and is illustrated on figure 3. This process is equivalent to the 215 steepest descent alternative of Braun and Willett (2013).
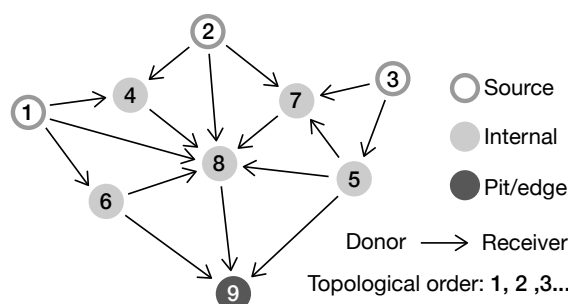
Do you mean multiple flow ?

Figure 3. DAG topology, illustrating the relationship between the different nodes int he graph (cells location). The arrows depicts individual relationships between a donor and one of its receiver. Node 9 is a *pit*, or *local minima*, if located inside the model grid and an *edge* if fluxes can escape from it. The topological ordering goes from the first node to be processed, to the last. Sources are nodes without donors.

3.2.1 Topological order for *implicit-lake*

The implicit lake solver is designed for cases where depressions are a secondary feature of the landscape evolution study. It ensures the flow continuity through the landscape and the conservation of original topography by connecting the pit of each depression to an outlet that will eventually reach the model edge (Cordonnier et al., 2018). It bypasses the computational

220 expense of explicitly solving lakes while still accounting for their existence. Our method is adapted from Cordonnier et al. (2018) to fit multiple-flow direction. In short, the algorithm links every node to either a single edge or a pit using a steepest descent route to define basins. It then links pairs of adjacent drainage basins using their lowest pair of cells and orders the basins via these connections from the most internal to the most external one. This defines for each internal basins which target cell needs to be the new receiver of the internal pits in order to ultimately drain to the edge.

225 Our implementation adds a couple of extra steps. First as mentioned in the previous section, our algorithm actually carves the elevation in the case of flat surfaces in order to avoid 0-slopes (see algorithm 3 in Cordonnier et al. (2018)). We make sure to reassess all the potential multiple-flow links impacted by this single-flow rerouting (e.g. cells from the target basin giving to the source basin). Once this step has been done, the topological order can be computed and will route flow through depression.

This methods has the advantage of speed, versatility and stability as demonstrated by the benchmarks of Cordonnier et al.

230 (2018). However, the links between basins is estimated with a steepest descent algorithm, which might shift the location of the geometrical outlet of the depression by a few pixels. It also maintains unconditional connectivity between local minima and their outlets, ignoring potential endhoreism.

3.2.2 Topological order for *explicit-lake*

The explicit lake solver aims to fully embrace the topographic complexity of depression systems. It does not assume the lakes

235 outflow and treats them as separate domains. The geometry of depression systems can be convoluted with multiple levels of subdepressions (Figure 4). To deal with this complexity, we build a binary trees for each depression system with a principle

adapted from Barnes et al. (2019): each vertex of the graphs can only have two children, and eventually one parent and one twin. It is built with a "vertical" logic illustrated on Figure 4 where each vertex correspond to a spatially identifiable domain made of a single or multiple merged depressions. Building such trees ensure efficient operations to numerically navigate through
240 individual depression systems (Barnes et al., 2019) and has been utilised for flooding landscapes with finite amount of water (Barnes et al., 2021). For simplicity, childless depressions are called a base depression, parentless depressions are called top depressions and the others intermediary depressions. Note that unique depressions are both childless and parentless.

We make heavy use of priority queue based algorithms to build the graph (see Barnes et al. (2014a) and Barnes et al. (2019) for full details about this data structure) which allows the dynamic sorting of selected cells function of their elevation. First we
245 emplace each internal pit cells in individual priority queues as starting point of all the base depressions and label the cell with a unique depression label (black dots on figure 4a). We process each priority queue until they are empty by popping out the lowest elevation cell and checking all of its neighbours. If the neighbour is higher in elevation, it is placed in the queue. The process is stopped when the depression is complete. For example if the current cell is already labelled with another depression index in which case both are labelled as twins and this cell represent their tipping node (e.g. depression 2 and 3 on figure 4a).
250 If one of the checked neighbours has a lower elevation, the cell is labeled as outlet and this depression will be the top one if not later labeled as twin. The trees are complete once all the priority queues are empty. Note that while we do not detail each and every one of them for the sake of clarity, the algorithm needs to manage a lot of potential edge cases. These are quite specific but to provide an example, one needs to make sure not to ignore any upstream neighbours of an outlet cell in case of future merging.
255 Our implementation only slightly differs from Barnes et al. (2019). The original algorithm is tuned for computing speed, we compute more information about each depression useful for the model:

- the volume of the depression V_{total}, note that it includes the volume of their children if any,

- the minimum volume of a depression (0 if base depression),

- a depression level, which represents the maximum distance in the tree from a base depression. Each base depression is
260 at level 0, and each parent's level is equal to the maximum level of their children plus 1,

- the tipping node of the depression, which represents either the outlet of the whole subsystem, or the node joining two twins

- the maximum elevation of the depression if filled.

In addition to these depression-specific information, the model stores a number of internal structures to navigate between
265 the DAG and the depression tree. Note that the maximum volume of water can include potential evaporation if enabled by the model, based on matrices Evaporation rates, E_{vl} (which are externally given to the model), summed over the maximum lake area.
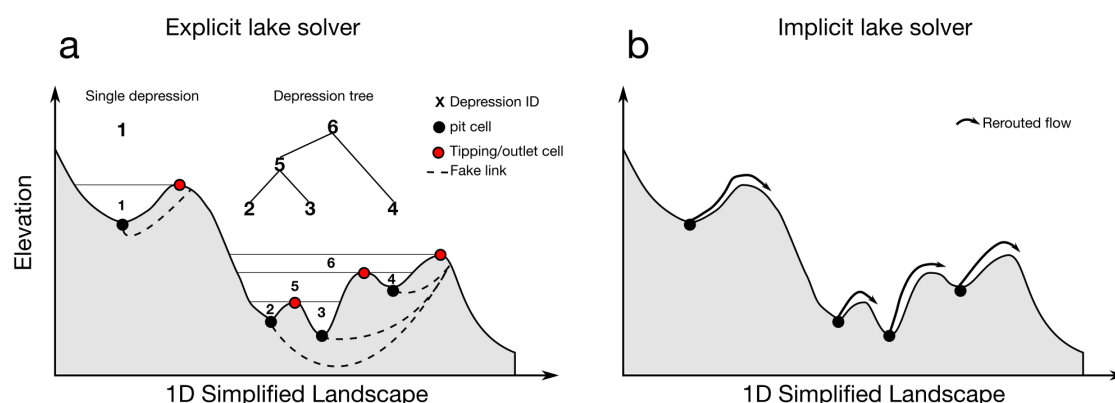
Figure 4. a) Cartoon illustrating the depression tree structure on a simplified 1D landscape. Each depression system has its own sub-tree, which can be as simple as a single-depression (e.g. depression 1). Dotted arrows represent fake temporary links used by the model to calculate an upstream/downstream direction despite the complex topography - the sole elevation value not being relevant in the case of local minima. b) Illustration of the implicit lake solver which reroutes flow using Cordonnier et al. (2018). Note how the flow is rerouted unconditionally to a model edge following a minimal cost path based on the elevation of the connections between each watersheds and the direct connection to the edge. For both a) and b) the landscape is represented in a simple 1D section. In 2D the problem becomes increasingly convoluted, especially if low-level noise or flat surfaces pollute the elevation.

Our depression tree rely on the principle of uniqueness of the tipping points which can be invalidated by numerically surfaces or if depression borders have equal elevation. To prevent this caveat, we add at each timestep a small numerical noise between -10^{-6} and 10^{-6} m and carve depressions with insignificant volumes using algorithm 3 of Cordonnier et al. (2018).

After building the depression tree, we can finally calculate the topological order for the explicit lake solver. This is achieved by temporarily linking in the DAG the pit cell of each base depressions to the cells downstream of the outlet of the top depression of each system which do not belonging to it figure 4a. These links are cancelled after the calculation of a topological order, but ensure that any lake system will be processed before its downstream counterparts.

3.3 Cellular-automata structure

3.3.1 Properties, parameterization and tracking

Once the DAG is built, the model skeleton is ready and a cell is built at each node. The information held by each cell can be adjusted and expanded on a needs basis. In the current implementation, cells have the following properties (illustrated in figure 2):

– Topographic elevation (in m)

11

- Thickness of the sediment layer (in m)

- Volumetric water flux Q_w in m^{3}yr^{-1} traversing the cell during a timestep

- Volumetric sediment flux Q_s in m^{3}yr^{-1} traversing the cell during a timestep (*mobile sediments*)

- Proportion of sediment flux from the fluvial system

285   - A list of receivers receiving either sediment or water from the cell, calculated from of the graph and from the process-law implemented in the model

- lists of weights describing the proportions of sediments and water transmitted to each receivers of the list

- erosion, sediment entertainment and deposition fluxes

- Tracking information if activated (e.g. proportion of the sediment flux coming from a given source area)

290   Some of these properties, like erosion or water for example, are reinitialised at each time step while others like topography or sediment thickness gets updated at each time step.

Three kinds of parameter inputs are currently available. First, external parameters which can be single values (e.g. dx, dy, dt), global arrays (e.g. 2D matrices of precipitation or uplift), spatially varying or even varying through time. Second, parameters that are label-dependent: a 2D matrix of labels defines discrete spatial areas and each label has a set of distinct parameters, for

295   example different rock-type can be associated with different erodibility and diffusivity (Gailleton, 2021). And third parameters that are fully dynamic: they are interdependent of each other and define by a function rather than a given value. Example of the latter are detailed in section 4.4.

The tracking capabilities of the method also relies on the labels. While the numerical implementation is tedious, its principle is simple: any material eroded by any processes from a location keeps track of its label as it is incorporated in the mobile

300   sediment flux. In the stratigraphy, a dynamic sparse matrix of cells stack "containers" of sediments also keeping track of the label proportions and allowing their remobilisation.

It is worth noting however, that this cellular-automata structure has some numerical limitation. To maintain all the advances detailed in this contribution, all the calculations needs to be processed from ridge to outlet, which is not necessarily compatible with all numerical laws. For example, solving the stream power like equations implicitly cannot necessarily be done with a

305   single downstream traversal of the landscape (e.g. Braun and Willett, 2013; Campforts et al., 2017; Hergarten et al., 2016). However they are not fully incompatible: one could imagine using the cellular automata method to post-process such model, only sacrificing the dynamic adjustment capabilities. But to begin offering such flexibility, we suggest that future effort should tend toward the development of a fully-fledged framework.

3.3.2 Cell processing order for local minima

310   The model processes the cells following the upstream-to-downstream topological order first assuming that there are no lakes. Before their turn, unprocessed cells "passively" receive water and sediments from upstream neighbours. When the cell is

the next in the topological order, the model applies external flux modifiers on it: precipitation, infiltration or any related process law affecting the water or sediment flux by adding/removing from external sources. Then the "active" process laws are executed in the following order: water routing; fluvial incision, deposition and sediment entrainment; and/or hillslope
315 diffusion following equations described in section 4.1 during which the weights of sediment and water splitting towards the cell's receivers are calculated. Finally, the "transport" processes transmit water and sediment to receiver cells, along with the proportion of sediment fluxes respectively belonging to hillslope and fluvial domains.

When the implicit lake solver is activated, lakes are not processed differently than the rest of the landscape, but cells in- claulated areas affected by flow rerouting have reduced topographic gradient and less direct connection to the rest of the
320 landscape, effectively simulating a "passive" landscape.   I do not understand.

Solving lakes explicitly is done in two steps. As it is not possible to know if we can fill or not a depression before having processed all the upstream cells in a "normal" way, a depression system is only processed once all its pit cells have received all the potential water and sediments. Only then the volume of water coming into the lake is used to fill it. This process can also account for evaporation.   What is it different from others LEMs solving lakes during a time step ?
325 The first step consists in calculating the total amount of water entering the full depression system by summing Q_w for each pit node of base depressions in the system. The tree is traversed from bottom to top, propagating the water from children to parents. In the end, the following volume of water $V_\mathrm{w\,in}$ enters each depression:

$$V_\mathrm{w\,in} = \sum_{i_\mathrm{pit}} Q_\mathrm{w}\,\Delta t\,, \tag{1}$$

where i_pit is the cell index of every pit cells downstream of a given depression.
330 The second step determine if the depression system needs breaking into sub-trees. The full tree is then assessed from the top depression. If the sum of available water is more than what the top depression can store, the whole lake system fills with water and will outflow. Otherwise if the minimum amount of water storable in the top depression is less than $V_\mathrm{w\,in}$, the lake does not outflow but all the children depressions will be filled. Finaly if the minimum amount of water storable in the top depression is greater than V_{wlin}, the local tree is divided in two and the assessment is reiterated until all the sub-trees are filled. Note that all
335 the water entering can eventually be evaporated, in which case no lake is created.

The third step consists in calculating the water elevation of the lake (h_w). Because our current implementation solves explicit finite difference schemes, we assume that, within a timestep, the volume of water the lake stores solely determines h_w — i.e., elevation changes due to lake sediment deposition are only applied at the end of the timestep. If the lake outflows, h_w equals the elevation of the outlet cell. Underfilled depressions lead to more complications (Garcia-Castellanos and Jiménez-Munt,
340 2015). In these cases, the model calculates a balance between lake evaporation and the available amount of water. Using a priority-queue based graph traversal (see section 3.2.2), we traverse the depression cells in increasing elevation order. Cells are included one by one and contribute in turn to storing the available amount of water $V_\mathrm{w\,avail}$ while giving their elevation to h_w:

$$V_\mathrm{w\,avail.} = V_\mathrm{w\,avail.} - N_\mathrm{lake}\,dx\,dy\,(\Delta z + Q_\mathrm{w\,evap})\,, \tag{2}$$

13

where N_{lake} tracks the number of cells already in the lake, Q_{evap} is water lost to evaporation, and Δz the elevation difference

345　between the current h_{w} and the elevation of the next node in the priority queue. The final h_{w} is calculated once $V_{\text{w avail.}} <$ $N_{\text{lake}}\, dx\, dy\, (\Delta z + Q_{\text{evap}})$.

3.3.3　Water and sediment fluxes into and across lakes

Once the water elevation is determined, the model back-calculates sediments. All the cells below water are "deprocessed" from continental processes: fluvial and hillslope processes are reversed with adequate correction on cells sediments and water con-

350　tents. The volume of sediment stored in the lake, $V_{\text{s in}}$, can now be stored in the lake straighfoforwardly as knows its final volume. Any excess is transmitted to the outlet cell. As noted by Garcia-Castellanos (2006) and Garcia-Castellanos and Jiménez-Munt (2015), the lake outlet needs particular care as its behavior through time ultimately controls the draining of a lake. Its deprocessing is only partial as it gives sediments to the lake and to the downstream landscape. Only the part of the fluxes going into the lake needs to be canceled and the other parts needs to be recalculated with the new amount of sediment and water. The

355　latter are determined by subtracting the incoming V_w and V_s by what has been stored. Additional care is needed to consider water and sediment coming to the outlet from its non-lacustrine upstream neighbours.

We cannot stress enough how convoluted this deprocessing can be, numerically speaking. One need to account carefully for all the neighbouring cells of the outlet and not remove/re-add fluxes multiple times. Given the critical nature of this task, we make sure our model is not plagued by uncovered edge cases and we implemented mass-balance checkers making sure no

360　water or sediments is lost due to the transfer processes. Mass-balance for a transferable flux can simply be defined as follow:

$$M = Q_{\text{in}} - Q_{\text{out}} \tag{3}$$

where Q_{in} encompasses any fluxes adding to the system and Q_{out} any fluxes leaving the system. For water flux, $Q_{\text{w in}}$ includes effective precipitations as well as water inherited from the lake in the previous time step (if lake are explicitly processed). $Q_{\text{w out}}$ encompasses any water stored in a lake at current time step, evaporation and water leaving the system via the model edges.

365　For sediment fluxes, $Q_{\text{s in}}$ includes any process removing material and putting it in transported flux (e.g. incision, entrainment, diffusion) and $Q_{\text{s out}}$ any processes depositing sediment from this flux (e.g. fluvial deposition, lake deposition) or exiting the model via the edges. The mass balance is respected if $M = 0$ (plus or minus numerical precision errors).

Finally, once all the cells have been processed, each cell applies its erosion and deposition fields to the topography and the sediment layer. The model also calculates and formats data to monitor the direct model outputs (e.g., maps of erosion, water

370　fluxes, sediment thickness), but also more indirect outputs such as the sum of the sediment fluxes outletting the model versus the sum of sediment fluxes stored in the sediment layers.

4 Application of the framework to new challenging scenarios

We demonstrate the capabilities of the method with three fields of applications. First we test the effect of considering lakes in a tectonically active range with an internal basin. Then we illustrate the tracking capabilities of the model monitoring the sediments flux coming from a magmatic pluton. Finally we explore the dynamic parametrisation feature with the same setting, adapting parameters function of the composition of the sediment flux. All the models starts from a same near-steady-state landscape obtained after running a simulation until drainage stabilisation with block uplift and non-subsiding foreland. The model has been tested on a computer with a intel i9-10980HK and 32 Gb or RAM on both MacOS Big Sur, Windows 10 and linux Ubuntu 22.04.

4.1 Process laws

To test the framework, we implemented a set of process laws that simulate long term hydrology, fluvial, and hillslope processes.

4.1.1 Hydrology

Hydrology in long-term landscape evolution model is usually approximated by flow routing algorithm distributing weighted drainage area from source nodes to outlets in the downstream direction, the weights representing the precipitation rates which can vary spatially (see Leonard and Whipple, 2021, for a comprehensive review on the subject). First local effective precipitation is added to the considered cell i:

$$Q_{i\,\mathrm{w}} = Q_{i\,\mathrm{w}} + P_i\,dx\,dy\,, \tag{4}$$

where P_i is the local effective precipitation weight factor that can include infiltration.

The second step is the routing to receivers. This can simply follow the steepest descent single flow direction (e.g. O'Callaghan and Mark, 1984; Braun and Willett, 2013) or a multiple flow direction (e.g. Tarboton, 1997; Schwanghart and Heckmann, 2012; Armitage, 2019). We implemented an adaptative algorithm routing water with multiple flow following the method from Bovy (2019). We added an optional parameter allowing the dynamic switching to single flow routing after an arbitrary threshold of discharge, to roughly simulate a transition from hillslope to fluvial domains. Note that we use relatively large cell sizes ($dx > 30$m) and this parameter is optional. In the multiple flow domain, water is split according to thee local slope. Following Bovy (2019), an exponent p is calculated for each receiver r of a cell i:

$$p_{\mathrm{r}} = 0.5 + 0.6\frac{dz}{dx} \tag{5}$$

and then normalised to satisfy $\sum p_\mathrm{r} = 1$ and conserve the mass balance. Then the water flux is transmitted to each receiver with:

$$Q_\mathrm{w} = Q_\mathrm{w} + Q_{i\,\mathrm{w}}^{p_\mathrm{r}} \tag{6}$$

400   4.1.2 fluvial erosion and deposition

We simulate fluvial erosion and deposition using the SPACE model (Shobe et al., 2017), a hybrid law allowing simultaneous treatment of detachment-limited and transport-limited portion of the rivers based on Davy and Lague (2009). It allows the processing of all kind of landscapes, whether sediments are absents or saturating the system and successfully collapses to both end-members under the right parameterisation. The process law separates sediment entrainment $^f E_s$, bedrock incision $^f E_r$
405   and sediment deposition $^f D_s$ into three equations solved simultaneously:

$$
\begin{aligned}
E_\mathrm{s} &= K_\mathrm{s} Q_\mathrm{w}^m S^n \left(1 - e^{-\frac{H}{H^*}}\right), \tag{7}\\
E_\mathrm{r} &= K_\mathrm{r} Q_\mathrm{w}^m S^n e^{-\frac{H}{H^*}}, \text{ and} \tag{8}\\
D_\mathrm{s} &= V \frac{Q_\mathrm{s}}{Q_\mathrm{w}}, \tag{9}
\end{aligned}
$$

where K_s is the sediment entrainment coefficient regulating the ease with which sediment cover can be mobilised; K_r the
410   erodibility coefficient ultimately controlling local rock strength (proxying various factors like weathering or fracturing); m and n are exponents regulating the relative importance of topographic gradient and water flux in the Stream Power Law (e.g. Harel et al., 2016); H is the sediment height; H^* is the bed roughness index linked the proportion of bedrock not covered by sediment; V is a dimensionless settling velocity coefficient encompassing information about the turbulence and composition of the suspended load. Details about all these parameters can be found in Shobe et al. (2017). In the case of multiple flow
415   departing from a single cell, the process is simply summed for each receivers: S, Q_w and Q_s being different for each.

4.1.3 Hillslope diffusion

Following the same philosophy, we implemented the non-linear hillslope diffusion of Carretier et al. (2016). This law separates sediment entrainment from deposition (i) allowing greater numerical stability than the purely non-linear explicit scheme (Roering et al., 1999) while (ii) keeping the non-local, non-linear aspect of the diffusion process. This law is versatile and collapses
420   to both linear and non-linear end members under different contexts as demonstrated in the original manuscript (Carretier et al., 2016). Material entrainment follow a local, straight-forward linear diffusion scheme which is defined as follow:

$$
\begin{aligned}
E_\mathrm{rock} &= \kappa_\mathrm{rock} \frac{dz}{dx} \tag{10}\\
E_\mathrm{soil} &= \kappa_\mathrm{soil} \frac{dz}{dx} \tag{11}
\end{aligned}
$$

where E_{rock} and E_{soil} are respectively the entrainment rate in [L/T] for bedrock and sediment; and κ_r and κ_s modulating

parameters function of the physical characteristic of the substrate and soil. Note that it is possible to disable bedrock diffusion

if one only considers soil movements. In the case of multiple flow, we respect the numerical implementation of Carretier et al.

(2016) considering that the steepest slope is the main driver to calculate $\frac{dz}{dx}$. If both E_{rock} and E_{soil} are active, E_{soil} is applied

first. If $E_{\text{soil}} * dt$ is greater than the soil thickness, remaining E_{rock} is applied proportionally to the remaining fraction of bedrock.

For example, if $E_{\text{soil}} * dt = 0.2m$ but soil thickness is 0.1, then E_{rock} is applied at 50%. Deposition of sediment by hillslope

processes is non-local and rely on a transport length approach based on Davy and Lague (2009):

$$D_{\text{hill}} = \frac{Q_s}{L} \text{ , where:} \tag{12}$$

$$L = \frac{dx\,dy}{1 - \left(\left(\frac{dz}{dx}\right)/S_c\right)^2} \tag{13}$$

where S_c is a critical slope parameter (Roering et al., 1999). if $dz/dx \ll S_c$, most of the sediments are deposited and we

approach the linear side of the equation. When $dz/dx \rightarrow S_c$, most of the sediment goes to the receivers as predicted by the

non-linear diffusion. In the case of $(dz/dx) > S_c$ then the process recasts the slope to S_c, adding any excess material to Q_s. A

conceptual difference with Carretier et al. (2016) is that we express volumetric flux rather than flux by unit width. This does not

affect the physical behavior of the process but is more consistent with the rest of our implementation. Q_s is modified according

to E_{rock}, E_{soil} and D_{hill} and fluxes are distributed to multiple receivers proportionally to the slope.

4.1.4 K and κ coefficients for erosion and sediment transport

The coefficients for hillslope and fluvial erosion or sediment transport — κ_s, κ_r, K_r and K_s — are empirical and their value

can greatly vary from a site to another (e.g Harel et al., 2016; Carretier et al., 2016). In stream-power-like models, they are

roughly function of m, n and local conditions. In hillslope diffusion, they are function of local soil and lithologically-driven

heterogeneity (Carretier et al., 2018). Because both of these empirical coefficients can encompass many processes (Tucker and

Slingerland, 1996; Whipple et al., 2013, e.g.), we use in this model a base value for each parameters which is common for the

whole landscape, or whole parts of the landscape, which we then modulate function of local heterogeneities or global patterns

of variations. While we still implemented the possibility to provide given values when physical processes and data allow direct

calculation of their absolute value (e.g Deal et al., 2018), this method allows more instinctive constraints. First, one can get a

rough idea of the base values by running sensitivity analysis and obtain relevant elevations, then one can apply dimensionless

and independent weighting coefficients function of the spatial variations to encompass in the simulation.

4.1.5 Lacustrine sedimentation

Give the parameter values of these simulation, cell size etc. A table would help.

Lake deposition is approximated with a simple draping algorithm. Once the final state of a lake is known (see section 3.2),

we calculate the proportion of the lake that can be filled with incoming sediment in each pixel: $V_{s\,\text{lake}}/(V_{\text{tot lake}}\,h_{\text{lake}})$. While

simplistic, it matches the aim of this contribution to act as a proof of concept in treating lakes as separate entities and paves the

way to more detailed lacustrine processes.

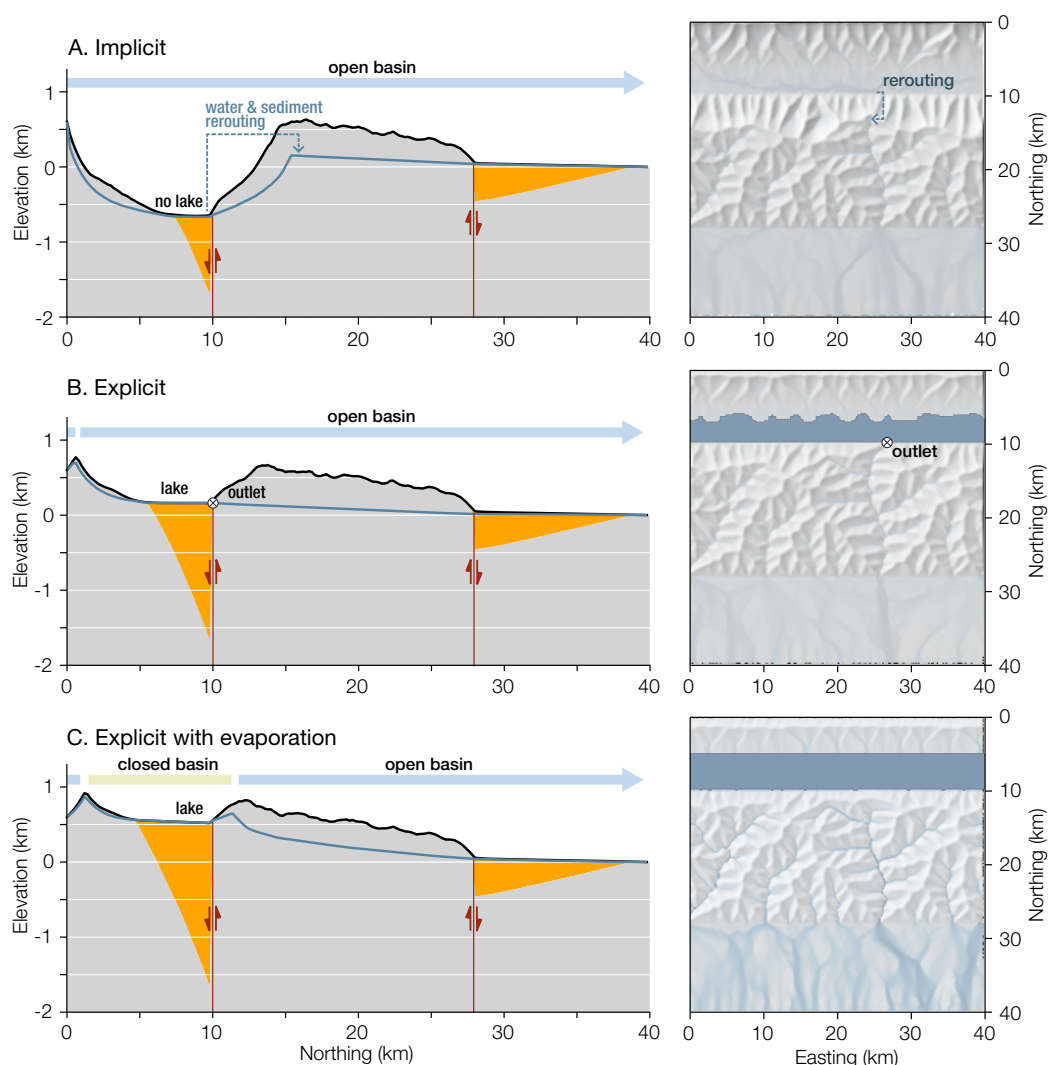455 **4.2   Application I: considering lakes in long-term landscapes evolution**

Figure 5. Resulting landscapes after 5 Myrs simulation for scenarios 1, 2a and 2b in A. B. and C. The left column displays N-S cross-sections of the median (black line) and minimum elevation (thin blue line) and the median sediment heigh (filled area in dim orange). The right column shows the extent of lakes (dark blue) and the water flux (lustreless blue) on a shaded topography. The minimum topography is a proxy for the elevation of the main river profiles, also highlighting a drainage divide for A and C. Note that only C has broken connectivity between internal basin and the foreland as A, by definition is unconditionally connected.

In this first set of experiments, we assess the role of lakes and closed basins in long-term landscapes evolution. Earlier work by Garcia-Castellanos (2006) and Garcia-Castellanos and Jiménez-Munt (2015) (respectively in 1D and 2D) already noted that endorheism in LEMs was function of complex relationship between climate (precipitation, evaporation), tectonics and surface processes. Their experiments highlighted the potential importance of integrating endhoreism in long term - large scale

460 landscape evolution studies. Here, we exploit our method's capacity to process lakes both explicitly and implicitly to assess how it could potentially impact results for a given setting.   quels sont les dimensions, paramètres de ces simulations ?

We ran three simulations for 10 Myrs in an idealized mountain range with a frontal thrust, a foreland, and a significant normal fault in its hinterland (figure 5) and a uniform semi-arid yearly precipitation rate of 700 mm. *Scenario 1* has the implicit lake solver (section 3.2.1), *scenario 2a* runs with the explicit lake solver (section 3.2.2) and *scenario 2b* has the explicit lake

465 solver with lake evaporation. Figure 5 displays a snapshot of the landscape after 5 Myrs as (i) a N-S median profile of median and minimum elevation and median sediment thickness and a hillshaded map-view of Q_w and lake extents; (ii) time series of sediment fluxes escaping the southern border of the model as well as the total volume of deposited sediment over the landscapes. Displaying the minimum elevation is equivalent to displaying the main river at each Northing location.

In *scenario 1*, an unrealistically deep (-500 m after 5 Myrs), underfilled and subsiding basin has formed on the footwall of the

470 normal fault. The main E-W drainage divide migrates significantly to the South (fig. 5 A). Over a total 10 Myr long evolution, the two basins store $4 \cdot 10^{11}$ m^3 of sediments while the exported sediment flux is only mildly impacted by the onset of the normal fault (fig. 6) and shows steady increase after 2 Myrs. In *scenario 2a*, using an explicit lake solver, sedimentation in the internal basin balances off subsidence. A long-lived very shallow lake is continuously connected to the foreland *via* a single river (fig. 5 B). The sediment export through time initially nearly halves from 4 to $2.5 \cdot 10^5$ m^3 yrs^{-1} as the depression grows and stabilises

475 beyond 3 Myrs (fig. 6). Finally in *scenario 2b* an internal, closed basin forms on the footwall of the normal fault (fig. 5C). Its elevation increases through time and it traps all the incoming sediments and water. It quickly becomes disconnected from the foreland as the blue linessets as described below must be submitted to specialized repositories. Please consider providing at

? least preliminary links to such assets for the period of minimum elevation shows (fig. 5C). The exported sediment flux halves from 4 to $2 \cdot 10^5$ m^3 yrs^{-1}, and increases again slightly and steadily through time (fig. 6).

480 Processing local minima is often overlooked in landscape evolution studies, nevertheless major differences emerge in the dynamic feedbacks affecting the sediment flux, the stratigraphy and topography. Changing the way local minima are solved affects both the ability of the internal basin to trap sediments and the connectivity within the landscapes.

In *scenario 1*, the internal depression is unconditionally connected to the rest of the outlet by the implicit lake solver and only fluvial deposition can fill the basin. The subsiding basin surface on fig. 5 A demonstrates fluvial deposition is not efficient

485 enough to balance the subsidence. If the topographic signature of the normal fault is exaggerated, fig. 6 show that its sediment flux signature is greatly attenuated (minor drop for 2 Myrs). More striking is the steady increase of sediment export, it can be explained by the constant lowering of the internal base level due to the inability of the basin to trap enough sediments: the internal landscape steepen, producing higher sediment volume, which are exported to the foreland due to the unconditional rerouting. Ultimately, if *scenario 1* ran for longer it would display a meaningless landscape inversion draining to the depocenter

490 of the internal basin and "teleporting" sediments to the model edge.

In Scenario 2a, the lake almost constantly outflows, maintaining connectivity to the foreland through the whole time. This is due to the large amount of water coming from the basin flanks compared to the accommodation space offered by the lake. The erosion of the outlet is *quasi* not impacted by the relatively small storage of water in the lake (this point is discussed in greater extents later in the discussion). This balance between maintaining the connection to the foreland base level but maintaining

495 the ability to trap sediment explains the stability of basin elevation (fig. 5 B) and sediment export through time (fig. 6) in equilibrium with the tectonic conditions. This results in very low actual lake depth ($< 1m$ most of the time), however this need to be interpreted bearing in mind the time step of our simulation is 1000 yrs and represent an average of processes in that time span. In reality, this could be translated in patches of migrating but more realistically deep lakes. More sophisticated acknowledgement of lake sediment dynamic like compaction could also enhance the creation of more realistic lakes (Håkanson,

500 1982).

Finally, *scenario 2b* is the only one breaking the connectivity to the rest of the landscapes, effectively simulating a closed basin. Lake evaporation balances water input in the lake and allows a decoupling where the would-be outlet of the lake does not receive any water or sediments from the lake, inhibiting its erosion compared to *scenario 2a*. The absence of outlet for the depression means all sediments are trapped in, explaining the highest volume of sediments stored and the lowest export to

505 the model edges. The elevation of the overall model also rises, and if ran for longer, the model would probably reach a steady state where the basin would connect to an external base level. The globally higher elevation and the increase of erosion export through time (fig. 6) results from the increasing elevation of the internal basin, effectively steepening the landscape, even on the foreland side.
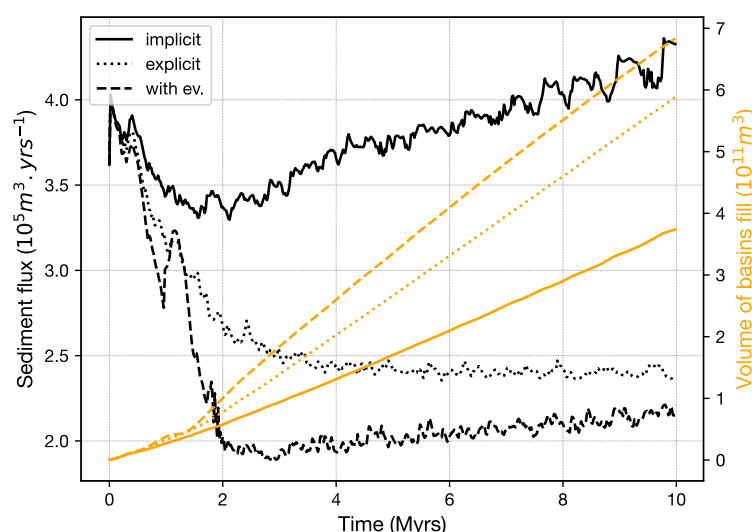

Figure 6. Sediment flux escaping the Southern boundary of the model (black) and stored in the landscape (dim orange) for scenario 1 (full line), 2 (dotted line) and 3 (dashed line).

4.3 Application II: Monitoring the source-to-sink system

510 This case demonstrates the ability of the CHONK method to provide fine-grained detailed information about the stratigraphy, in term of provenance data. LEMs have been widely used to investigate the source-to-sink systems (e.g. Guerit et al., 2019; Yuan et al., 2019; Sharman et al., 2019). One particular need of source-to-sink is the ability to track the provenance and the destiny of material during their erosion transport and sedimentation processes. This can be done by tracking discrete individual particles (Carretier et al., 2016), or with a bulk approach (Sharman et al., 2019). The latter usually post-processes this information by

515 integrating the erosion and sedimentation field. Our approach allows an easy embedding of such information within the cell. The tracking of provenance is built-in and straightforward. it also enable the addition of more details: the provenance can be tracked within the stratigraphy and reutilised in later timestep without information loss. We demonstrate the model capabilities with a run similar to *scenario 2* from section 4.2, but exhuming a simple pluton-like of harder rock type in the range. Greater rock strength was simulated with a decrease in erodibility. We refer to the harder rock type as granite and the background rock

520 type as substrate for simplicity.

We ran the simulation for 10 Myrs and illustrate different ways we can monitor the results on fig 7. Fig 7 a illustrates the high-resolution monitoring of the sediment flux with a granite provenance can be found. Thanks to the 3D cellular system storing this information, it can be retrieved with different resolutions, for example in the full sediment column or in the first 10 m as illustrated on fig 7a. The latter also shows how one can quickly define the extent of a provenance signature within basins,

525 and whether it is fully captured (like in the internal basin) or localised along flow paths, like in the foreland basin. fig 7b and c display this information in cross-section view. This can be particularly useful to investigate large-scale stratigraphic structure. Note that it displays the provenance data as relative proportion instead of absolute volume in this case, both are possible and holding different type of information. The E-W and N-S cross-sections in figure 7 illustrate the irregularity in the stratigraphic patterns of deposition as the distributary system sweeps across the foreland.

530 4.4 Application III: Erosivity and erodibility captured by dynamic parameters

If the tracking capabilities offer large possibilities in terms of monitoring the source-to-sink system, they can also be used to integrate feedbacks between processes and characteristics of the sediment flux. Because the tracking is dynamic, the state of the fluxes is always known and one can use it to influence directly the process laws. In the following example, we alter the K coefficients of erosion efficency in equations 8 and 7 to incorporate a notion of relative strengths between sediment

535 and substrate. In short, we assume that harder tools (e.g. granite) impacting softer bedrock (e.g. mudstone) yield greater river incision than softer tools (e.g. schist) on harder material (e.g. Sklar and Dietrich, 1998; Sklar, 2001; Sklar and Dietrich, 2004). We take advantage of the dynamic parametrisation of CHONK to implement a first-order tool strength principle: *that's really new*

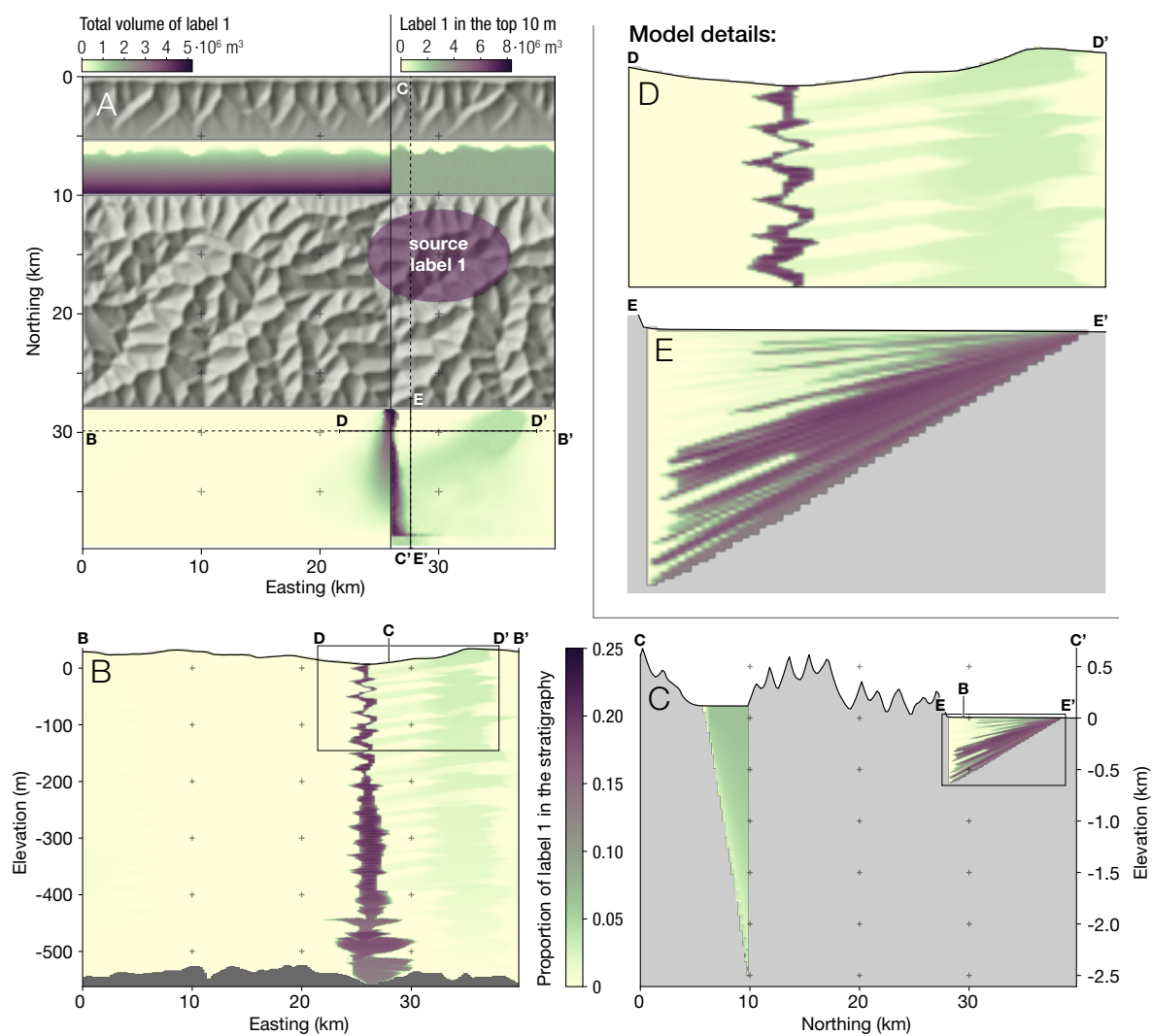$$K_{\text{eff}} = \frac{K_{\text{r}}}{K_{\text{sed}}}^{s} * K_i \tag{14}$$

21

Figure 7. Provenance of sediments after 10 Myrs, expressed in proportions or volume of sediment coming from the granitoid (dark purple).

where K_{eff} is the effective erodibility used in the equation, K_{r} is the bedrock erodibility, K_{sed} is the erodibility of the mobile
540 sediment, s is an exponent regulating the sensitivity of the system and K_i is the local erodibility factor. K_{sed} is calculated

what are the parameters values of Equation 14 in this simulation ? (s, Ksed etc…)

proportionally to the content of each lithologies in the model.

We ran a modified simulation with an uplifting range and a static foreland, essentially fig. 7 A without the normal fault.
We start from steady-state conditions and exhume a simplified granitoid. Fig. 8 shows a snapshot of the main river draining
through the granitoid at t=0 and t=3 Myrs for an unmodified simulation using equation 8 and the tool effect simulation using
545 equation 14 to highlight non-linear and non-local effects. With hard tool enhancing incision, the area downstream of the harder
rocks lowers its base level which will propagate knickpoints up tributaries, regardless of their lithology. Because this enhanced
incision is function of the quantity of granite in the mobile sediments, its effect fades downstream as more softer sediment
adds in the mobile flux, affecting the non-linearly the concavity of the river profile. In the granitoid-bearing area, the reduced
erosional efficiency of soft sediment on a harder bed leads to a steeper river reach.
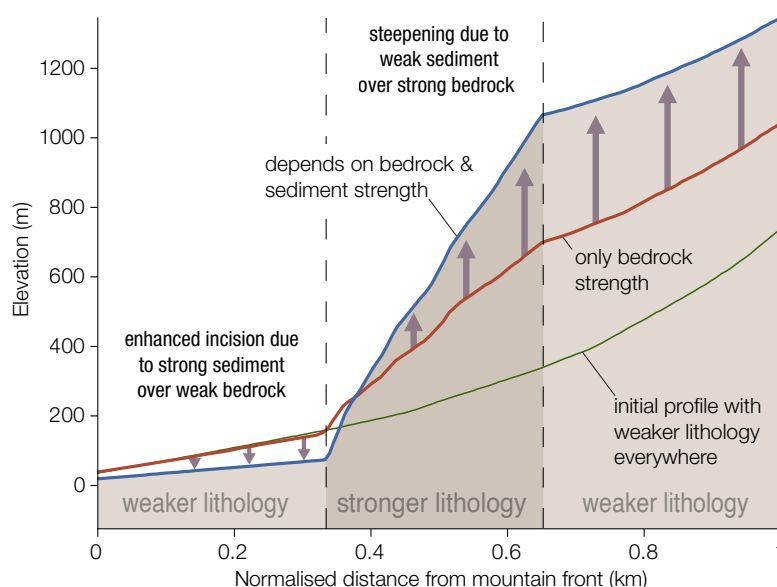

Figure 8. River long profiles normalised to mountain front for the initial topography (light green) and the simulation with and without the
modified equation 14 (respectively in blue and red). The initial profile was near equilibrium with homogeneous lithology, hence is unaffected
by the modified equation. Note how the differences are not only localised within the harder rock area but also in the downstream part as well,
illustrating a strong non-local component.

5 Discussions and conclusions

You have to better convince why previous models are not cellular-automata (I think they are). See Tucker and Hancock (2010).

In this contribution we explored the potential of this method and illustrated it with three simple applications. The main advantages of expressing LEM into a cellular-automata framework are that (i) it is built for interoperability between fluxes and parameters and (ii) it allows fine-grained monitoring of fluxes independently from surface laws, making it a prime tool for source-to-sink and other sedimentological or stratigraphic studies. Crossing it with graph theories enables full and efficient control of topology, even in region where imbrications of local minimas complicate it significantly. Whether lakes, endhoreic basins or unsignificant noise, our method can process local minima with a lot of flexibility depending on the case study. They can be treated as fully separated domains with dedicated process laws and/or act as partial or full trap in the source-to-sink sediment and water routine. Local minima can also be simply rerouted to ensure flow continuity without affecting computing performances or requiring dedicated processes. Often overlooked or bypassed, we demonstrated that the way local minima are integrated into the model significantly impacts the simulated landscape evolution. Our approach is built upon existing contributions (e.g. Garcia-Castellanos et al., 2003; Garcia-Castellanos and Jiménez-Munt, 2015), and its main breakthrough

is ? the generic processing of these closed domains independent from process-laws. This allows a seamless integration within landscape evolution models.

The dynamic nature of the model enables advanced tracking capabilities. These can be used to monitor sediment provenance, store and reuse tracking information in the stratigraphy, or use it to influence process law. While we focused on the provenance, this opens a wide range of possibilities linked to any information that can be tracked in the cells. For example, one could extend this provenance information to geochemical tracers, or detrial thermochronometer and cosmonuclides. In the end, a tracker just needs to be associated with its transporting flux whether hillslope or fluvial sediment or water. Another field of possibility is the tracking of more indirect properties, such as residence time which are crucial to model luminescence and cosmogenic signals.

Code availability. The model prototype is open-source and available in a github repository (https://github.com/bgailleton/CHONK) with instruction about usage and installation.

References

Adams, J. M., Gasparini, N. M., Hobley, D. E. J., Tucker, G. E., Hutton, E. W. H., Nudurupati, S. S., and Istanbulluoglu, E.: The Land-lab v1.0 OverlandFlow component: a Python tool for computing shallow-water flow across watersheds, Geoscientific Model Develop-ment, 10, 1645–1663, https://doi.org/10.5194/gmd-10-1645-2017, https://gmd.copernicus.org/articles/10/1645/2017/, publisher: Coperni-cus GmbH, 2017.

Anand, S. K., Hooshyar, M., and Porporato, A.: Linear layout of multiple flow-direction networks for landscape-evolution simulations, En-vironmental Modelling & Software, 133, 104 804, https://doi.org/10.1016/j.envsoft.2020.104804, https://www.sciencedirect.com/science/article/pii/S1364815220305934, 2020.

Armitage, J. J.: Short communication: Flow as distributed lines within the landscape, Earth Surface Dynamics, 7, 67–75, https://doi.org/10.5194/esurf-7-67-2019, publisher: Copernicus GmbH, 2019.

Babault, J., Bonnet, S., Crave, A., and Van Den Driessche, J.: Influence of piedmont sedimentation on erosion dynamics of an uplifting landscape: An experimental approach, Geology, 33, 301–304, https://doi.org/10.1130/G21095.1, https://doi.org/10.1130/G21095.1, 2005.

Barnes, R., Lehman, C., and Mulla, D.: An efficient assignment of drainage direction over flat surfaces in raster digital elevation models, Computers & Geosciences, 62, 128–135, https://doi.org/10.1016/j.cageo.2013.01.009, https://www.sciencedirect.com/science/article/pii/S009830041300023X, 2014a.

Barnes, R., Lehman, C., and Mulla, D.: Priority-flood: An optimal depression-filling and watershed-labeling algorithm for digital el-evation models, Computers and Geosciences, 62, 117–127, https://doi.org/10.1016/j.cageo.2013.04.024, publisher: Pergamon _eprint: 1511.04463, 2014b.

Barnes, R., Callaghan, K. L., and Wickert, A. D.: Computing water flow through complex landscapes, Part 2: Finding hierarchies in depres-sions and morphological segmentations, Computing water flow through complex landscapes, Part 2: Finding hierarchies in depressions and morphological segmentations, pp. 1–19, https://doi.org/10.5194/esurf-2019-34, 2019.

Barnes, R., Callaghan, K. L., and Wickert, A. D.: Computing water flow through complex landscapes – Part 3: Fill–Spill–Merge: flow routing in depression hierarchies, Earth Surface Dynamics, 9, 105–121, https://doi.org/10.5194/esurf-9-105-2021, https://esurf.copernicus.org/articles/9/105/2021/, publisher: Copernicus GmbH, 2021.

Barnhart, K. R., Glade, R. C., Shobe, C. M., and Tucker, G. E.: Terrainbento 1.0: a Python package for multi-model analysis in long-term drainage basin evolution, Geoscientific Model Development, 12, 1267–1297, https://doi.org/10.5194/gmd-12-1267-2019, https://gmd.copernicus.org/articles/12/1267/2019/, 2019.

Barnhart, K. R., Hutton, E. W. H., Tucker, G. E., Gasparini, N. M., Istanbulluoglu, E., Hobley, D. E. J., Lyons, N. J., Mouchene, M., Nudurupati, S. S., Adams, J. M., and Bandaragoda, C.: Short communication: Landlab v2.0: a software package for Earth surface dy-namics, Earth Surface Dynamics, 8, 379–397, https://doi.org/10.5194/esurf-8-379-2020, https://esurf.copernicus.org/articles/8/379/2020/, publisher: Copernicus GmbH, 2020.

Bates, P. D., Horritt, M. S., and Fewtrell, T. J.: A simple inertial formulation of the shallow water equations for efficient two-dimensional flood inundation modelling, Journal of Hydrology, 387, 33–45, https://doi.org/10.1016/j.jhydrol.2010.03.027, https://www.sciencedirect.com/science/article/pii/S0022169410001538, 2010.

Bovy, B.: fastscape-lem/fastscape: v0.1.0alpha, https://doi.org/10.5281/ZENODO.3479426, 2019.

Braun, J. and Sambridge, M.: Modelling landscape evolution on geological time scales: a new method based on irregular spatial discretization, Basin Research, 9, 27–52, https://doi.org/10.1046/j.1365-2117.1997.00030.x, https://onlinelibrary.wiley.com/doi/abs/10.1046/j.1365-2117.1997.00030.x, _eprint: https://onlinelibrary.wiley.com/doi/pdf/10.1046/j.1365-2117.1997.00030.x, 1997.

615 Braun, J. and Willett, S. D.: A very efficient O(n), implicit and parallel method to solve the stream power equation governing fluvial incision and landscape evolution, Geomorphology, 180-181, 170–179, https://doi.org/10.1016/j.geomorph.2012.10.008, 2013.

Bufe, A., Burbank, D. W., Liu, L., Bookhagen, B., Qin, J., Chen, J., Li, T., Thompson Jobe, J. A., and Yang, H.: Variations of Lateral Bedrock Erosion Rates Control Planation of Uplifting Folds in the Foreland of the Tian Shan, NW China, Journal of Geophysical Research, 122, 2431–2467, 2017.

620 Campforts, B., Schwanghart, W., and Govers, G.: Accurate simulation of transient landscape evolution by eliminating numerical diffusion: The TTLEM 1.0 model, Earth Surface Dynamics, 5, 47–66, https://doi.org/10.5194/esurf-5-47-2017, 2017.

Campforts, B., Shobe, C. M., Steer, P., Vanmaercke, M., Lague, D., and Braun, J.: HyLands 1.0: a hybrid landscape evolution model to simulate the impact of landslides and landslide-derived sediment on landscape evolution, Geoscientific Model Development, 13, 3863–3886, https://doi.org/10.5194/gmd-13-3863-2020, https://gmd.copernicus.org/articles/13/3863/2020/, publisher: Copernicus GmbH, 2020.

625 Carretier, S., Martinod, P., Reich, M., and Godderis, Y.: Modelling sediment clasts transport during landscape evolution, Earth Surface Dynamics, 4, 237–251, https://doi.org/10.5194/esurf-4-237-2016, https://esurf.copernicus.org/articles/4/237/2016/, publisher: Copernicus GmbH, 2016.

Carretier, S., Goddéris, Y., Martinez, J., Reich, M., and Martinod, P.: Colluvial deposits as a possible weathering reservoir in uplifting mountains, Earth Surface Dynamics, 6, 217–237, https://doi.org/10.5194/esurf-6-217-2018, https://esurf.copernicus.org/articles/6/217/2018/,
630 publisher: Copernicus GmbH, 2018.

Clift, P. D. and Giosan, L.: Sediment fluxes and buffering in the post-glacial Indus Basin, Basin Research, 26, 369–386, 2014.

Cordonnier, G., Bovy, B., and Braun, J.: A Versatile, Linear Complexity Algorithm for Flow Routing in Topographies with Depressions, Earth Surface Dynamics Discussions, 7, 1–18, https://doi.org/10.5194/esurf-2018-81, publisher: Copernicus GmbH, 2018.

Coulthard, T., Neal, J., Bates, P., Ramirez, J., De Almeida, G., and Hancock, G.: Integrating the LISFLOOD-FP 2D hydrodynamic
635 model with the CAESAR model: implications for modelling landscape evolution, Earth Surface Processes and Landforms, 38, https://doi.org/10.1002/esp.3478, 2013.

Croissant, T., Lague, D., Steer, P., and Davy, P.: Rapid post-seismic landslide evacuation boosted by dynamic river width, Nature Geoscience, 10, 680–684, https://doi.org/10.1038/ngeo3005, https://doi.org/10.1038/ngeo3005, 2017.

D'Ambrosio, D., Di Gregorio, S., Gabriele, S., and Gaudio, R.: A Cellular Automata model for soil erosion by water, Physics and
640 Chemistry of the Earth, Part B: Hydrology, Oceans and Atmosphere, 26, 33–39, https://doi.org/10.1016/S1464-1909(01)85011-5, https://www.sciencedirect.com/science/article/pii/S1464190901850115, 2001.

Davy, P. and Lague, D.: Fluvial erosion/transport equation of landscape evolution models revisited, Journal of Geophysical Research: Solid Earth, 114, https://doi.org/10.1029/2008JF001146, publisher: Blackwell Publishing Ltd, 2009.

Davy, P., Croissant, T., and Lague, D.: A precipiton method to calculate river hydrodynamics, with applications to flood predic-
645 tion, landscape evolution models, and braiding instabilities, Journal of Geophysical Research: Earth Surface, 122, 1491–1512, https://doi.org/10.1002/2016JF004156, 2017.

Deal, E., Braun, J., and Botter, G.: Understanding the Role of Rainfall and Hydrology in Determining Fluvial Erosion Efficiency, Journal of Geophysical Research: Earth Surface, 123, 744–778, https://doi.org/10.1002/2017JF004393, https://onlinelibrary.wiley.com/doi/abs/10.1002/2017JF004393, _eprint: https://onlinelibrary.wiley.com/doi/pdf/10.1002/2017JF004393, 2018.

650   Dingle, E. H., Sinclair, H. D., Venditti, J. G., Attal, M., Kinnaird, T. C., Creed, M., Quick, L., Nittrouer, J. A., and Gautam, D.:
Sediment dynamics across gravel-sand transitions: Implications for river stability and floodplain recycling, Geology, 48, 468–472,
https://doi.org/10.1130/G46909.1, https://doi.org/10.1130/G46909.1, 2020.

Finnegan, N. J., Sklar, L. S., and Fuller, T. K.: Interplay of sediment supply, river incision, and channel morphology re-
vealed by the transient evolution of an experimental bedrock channel, Journal of Geophysical Research: Earth Surface, 112,

655   https://doi.org/https://doi.org/10.1029/2006JF000569, https://agupubs.onlinelibrary.wiley.com/doi/abs/10.1029/2006JF000569, 2007.

Gailleton, B.: fastscape-lem/fastscape-litho: fastscape-litho 0.0.1, https://doi.org/10.5281/zenodo.4773791, https://zenodo.org/record/
4773791, 2021.

Gailleton, B., Sinclair, H. D., Mudd, S. M., Graf, E. L. S., and Maṭenco, L. C.: Isolating Lithologic Versus Tectonic Signals of River
Profiles to Test Orogenic Models for the Eastern and Southeastern Carpathians, Journal of Geophysical Research: Earth Surface,

660   126, e2020JF005 970, https://doi.org/10.1029/2020JF005970, https://onlinelibrary.wiley.com/doi/abs/10.1029/2020JF005970, _eprint:
https://onlinelibrary.wiley.com/doi/pdf/10.1029/2020JF005970, 2021.

Ganti, V., Straub, K. M., Foufoula-Georgiou, E., and Paola, C.: Space-time dynamics of depositional systems: Experimental evidence and the-
oretical modeling of heavy-tailed statistics, Journal of Geophysical Research: Earth Surface, 116, https://doi.org/10.1029/2010JF001893,
https://onlinelibrary.wiley.com/doi/abs/10.1029/2010JF001893, _eprint: https://onlinelibrary.wiley.com/doi/pdf/10.1029/2010JF001893,

665   2011.

Garcia-Castellanos, D.: Long-term evolution of tectonic lakes: Climatic controls on the development of internally
drained basins, https://doi.org/10.1130/2006.2398(17), https://pubs.geoscienceworld.org/gsa/books/book/569/chapter/3803150/
Long-term-evolution-of-tectonic-lakes-Climatic, 2006.

Garcia-Castellanos, D. and Jiménez-Munt, I.: Topographic Evolution and Climate Aridification during Continental Collision: Insights

670   from Computer Simulations, PLOS ONE, 10, e0132 252, https://doi.org/10.1371/journal.pone.0132252, https://journals.plos.org/plosone/
article?id=10.1371/journal.pone.0132252, publisher: Public Library of Science, 2015.

Garcia-Castellanos, D., Vergés, J., Gaspar-Escribano, J., and Cloetingh, S.: Interplay between tectonics, climate, and flu-
vial transport during the Cenozoic evolution of the Ebro Basin (NE Iberia), Journal of Geophysical Research: Solid
Earth, 108, https://doi.org/10.1029/2002JB002073, https://onlinelibrary.wiley.com/doi/abs/10.1029/2002JB002073, _eprint:

675   https://onlinelibrary.wiley.com/doi/pdf/10.1029/2002JB002073, 2003.

Geurts, A. H., Cowie, P. A., Duclaux, G., Gawthorpe, R. L., Huismans, R. S., Pedersen, V. K., and Wedmore, L. N. J.: Drainage integration
and sediment dispersal in active continental rifts: A numerical modelling study of the central Italian Apennines, Basin Research, 30, 965–
989, https://doi.org/10.1111/bre.12289, https://www.earthdoc.org/content/journals/10.1111/bre.12289, publisher: European Association
of Geoscientists & Engineers, 2018.

680   Grieve, S. W., Mudd, S. M., Milodowski, D. T., Clubb, F. J., and Furbish, D. J.: How does grid-resolution modulate the topographic expression
of geomorphic processes?, Earth Surface Dynamics, 4, 627–653, https://doi.org/10.5194/esurf-4-627-2016, publisher: Copernicus GmbH,
2016.

Guerit, L., Métivier, F., Devauchelle, O., Lajeunesse, E., and Barrier, L.: Laboratory alluvial fans in one dimension, Physical Review E, 90,
022 203, https://doi.org/10.1103/PhysRevE.90.022203, https://link.aps.org/doi/10.1103/PhysRevE.90.022203, publisher: American Phys-

685   ical Society, 2014.

Guerit, L., Yuan, X.-P., Carretier, S., Bonnet, S., Rohais, S., Braun, J., and Rouby, D.: Fluvial landscape evolution controlled by the sediment deposition coefficient: Estimation from experimental and natural landscapes, Geology, 47, 853–856, https://doi.org/10.1130/g46356.1, publisher: Geological Society of America, 2019.

Harel, M. A., Mudd, S. M., and Attal, M.: Global analysis of the stream power law parameters based on worldwide 10 Be denudation rates, Geomorphology, 268, 184–196, https://doi.org/10.1016/j.geomorph.2016.05.035, 2016.

Hergarten, S.: Transport-limited fluvial erosion – simple formulation and efficient numerical treatment, Earth Surface Dynamics, 8, 841–854, https://doi.org/10.5194/esurf-8-841-2020, https://esurf.copernicus.org/articles/8/841/2020/, publisher: Copernicus GmbH, 2020.

Hergarten, S., Robl, J., and Stuwe, K.: Tectonic geomorphology at small catchment sizes-extensions of the stream-power approachand the x method, Earth Surface Dynamics, 4, 1–9, https://doi.org/10.5194/esurf-4-1-2016, publisher: Copernicus GmbH, 2016.

HOWARD, A. D. and KERBY, G.: Channel changes in badlands, GSA Bulletin, 94, 739–752, https://doi.org/10.1130/0016-7606(1983)94<739:CCIB>2.0.CO;2, https://doi.org/10.1130/0016-7606(1983)94<739:CCIB>2.0.CO;2, _eprint: https://pubs.geoscienceworld.org/gsabulletin/article-pdf/94/6/739/3434551/i0016-7606-94-6-739.pdf, 1983.

Håkanson, L.: Bottom dynamics in lakes, in: Sediment/Freshwater Interaction, edited by Sly, P. G., Developments in Hydrobiology, pp. 9–22, Springer Netherlands, Dordrecht, https://doi.org/10.1007/978-94-009-8009-9_2, 1982.

Jerolmack, D. J. and Sadler, P.: Transience and persistence in the depositional record of continental margins, Journal of Geophysical Research: Earth Surface, 112, https://doi.org/10.1029/2006JF000555, https://onlinelibrary.wiley.com/doi/abs/10.1029/2006JF000555, _eprint: https://onlinelibrary.wiley.com/doi/pdf/10.1029/2006JF000555, 2007.

Jyotsna, R. and Haff, P. K.: Microtopography as an indicator of modern hillslope diffusivity in arid terrain, Geology, 25, 695–698, https://doi.org/10.1130/0091-7613(1997)025<0695:MAAIOM>2.3.CO;2, https://pubs.geoscienceworld.org/gsa/geology/article-abstract/25/8/695/189088/Microtopography-as-an-indicator-of-modern, publisher: GeoScienceWorld, 1997.

L. Callaghan, K. and D. Wickert, A.: Computing water flow through complex landscapes - Part 1: Incorporating depressions in flow routing using FlowFill, Earth Surface Dynamics, 7, 737–753, https://doi.org/10.5194/esurf-7-737-2019, publisher: Copernicus GmbH, 2019.

Leonard, J. S. and Whipple, K. X.: Influence of Spatial Rainfall Gradients on River Longitudinal Profiles and the Topographic Expression of Spatially and Temporally Variable Climates in Mountain Landscapes, Journal of Geophysical Research: Earth Surface, 126, e2021JF006 183, https://doi.org/10.1029/2021JF006183, https://onlinelibrary.wiley.com/doi/abs/10.1029/2021JF006183, _eprint: https://onlinelibrary.wiley.com/doi/pdf/10.1029/2021JF006183, 2021.

Lindsay, J. B.: Efficient hybrid breaching-filling sink removal methods for flow path enforcement in digital elevation models, Hydrological Processes, 30, 846–857, https://doi.org/10.1002/hyp.10648, publisher: Wiley-Blackwell, 2016.

Lupker, M., Lavé, J., France-Lanord, C., Christl, M., Bourlès, D., Carcaillet, J., Maden, C., Wieler, R., Rahman, M., Bezbaruah, D., and Xiaohan, L.: [10]Be systematics in the Tsangpo-Brahmaputra catchment: the cosmogenic nuclide legacy of the eastern Himalayan syntaxis, Earth Surface Dynamics, 5, 429–449, https://doi.org/10.5194/esurf-5-429-2017, https://esurf.copernicus.org/articles/5/429/2017/, 2017.

Malatesta, L. C. and Avouac, J.-P.: Contrasting river incision in north and south Tian Shan piedmonts due to variable glacial imprint in mountain valleys, Geology, 46, 659–662, https://doi.org/10.1130/G40320.1, https://doi.org/10.1130/G40320.1, 2018.

Malatesta, L. C., Avouac, J.-P., Brown, N. D., Breitenbach, S. F. M., Pan, J., Chevalier, M.-L., Rhodes, E., Saint-Carlier, D., Zhang, W., Charreau, J., Lavé, J., and Blard, P.-H.: Lag and mixing during sediment transfer across the Tian Shan piedmont caused by climate-driven aggradation–incision cycles, Basin Research, 30, 613–635, https://doi.org/https://doi.org/10.1111/bre.12267, https://onlinelibrary.wiley.com/doi/abs/10.1111/bre.12267, 2018.

Mudd, S. M., Clubb, F. J., Grieve, S. W. D., Milodowski, D. T., Hurst, M. D., Gailleton, B., and Valters, D. A.: LSDTopoTools2,
725   https://doi.org/10.5281/ZENODO.3245041, 2019.

Nagel, K. and Schreckenberg, M.: A cellular automaton model for freeway traffic, Journal de Physique I, 2, 2221–2229,
    https://doi.org/10.1051/jp1:1992277, http://dx.doi.org/10.1051/jp1:1992277, publisher: EDP Sciences, 1992.

O'Callaghan, J. F. and Mark, D. M.: The extraction of drainage networks from digital elevation data., Computer Vision, Graphics, & Image
    Processing, 28, 323–344, https://doi.org/10.1016/S0734-189X(84)80011-0, publisher: Elsevier, 1984.

730   Paola, C., Straub, K., Mohrig, D., and Reinhardt, L.: The "unreasonable effectiveness" of stratigraphic and geomorphic experiments, Earth-
    Science Reviews, 97, 1–43, 2009.

Perron, J. T.: Numerical methods for nonlinear hillslope transport laws, Journal of Geophysical Research: Earth Sur-
    face, 116, https://doi.org/10.1029/2010JF001801, https://agupubs.onlinelibrary.wiley.com/doi/abs/10.1029/2010JF001801, _eprint:
    https://agupubs.onlinelibrary.wiley.com/doi/pdf/10.1029/2010JF001801, 2011.

735   Roelvink, J. and Van Banning, G.: Design and development of DELFT3D and application to coastal morphodynamics, Oceanographic
    Literature Review, 11, 925, 1995.

Roering, J. J., Kirchner, J. W., and Dietrich, W. E.: Evidence for nonlinear, diffusive sediment transport on hillslopes and implications for
    landscape morphology, Water Resources Research, 35, 853–870, https://doi.org/10.1029/1998WR900090, 1999.

Sadler, P. M.: Sediment Accumulation Rates and the Completeness of Stratigraphic Sections, The Journal of Geology, 89, 569–584,
740   https://doi.org/10.1086/628623, https://www.journals.uchicago.edu/doi/abs/10.1086/628623, publisher: The University of Chicago Press,
    1981.

Salles, T.: eSCAPE: Regional to Global Scale Landscape Evolution Model v2.0, Geoscientific Model Development, 12, 4165–4184,
    https://doi.org/10.5194/gmd-12-4165-2019, https://gmd.copernicus.org/articles/12/4165/2019/, publisher: Copernicus GmbH, 2019.

Salles, T., Lopez, S., Cacas, M. C., and Mulder, T.: Cellular automata model of density currents, Geomorphology, 88, 1–20,
745   https://doi.org/10.1016/j.geomorph.2006.10.016, https://www.sciencedirect.com/science/article/pii/S0169555X06004648, 2007.

Schumer, R., Taloni, A., and Furbish, D. J.: Theory connecting nonlocal sediment transport, earth surface roughness, and the Sadler effect,
    Geophysical Research Letters, 44, 2281–2289, https://doi.org/10.1002/2016GL072134, https://onlinelibrary.wiley.com/doi/abs/10.1002/
    2016GL072134, _eprint: https://onlinelibrary.wiley.com/doi/pdf/10.1002/2016GL072134, 2017.

Schwanghart, W. and Heckmann, T.: Fuzzy delineation of drainage basins through probabilistic interpretation of diverging flow algo-
750   rithms, Environmental Modelling & Software, 33, 106–113, https://doi.org/10.1016/j.envsoft.2012.01.016, https://www.sciencedirect.
    com/science/article/pii/S1364815212000345, 2012.

Schwanghart, W. and Kuhn, N. J.: TopoToolbox: A set of Matlab functions for topographic analysis, Environmental Modelling and Software,
    25, 770–781, https://doi.org/10.1016/j.envsoft.2009.12.002, 2010.

Schwanghart, W. and Scherler, D.: Short Communication: TopoToolbox 2 - MATLAB-based software for topographic analysis and modeling
755   in Earth surface sciences, Earth Surface Dynamics, 2, 1–7, https://doi.org/10.5194/esurf-2-1-2014, 2014.

Sharman, G. R., Sylvester, Z., and Covault, J. A.: Conversion of tectonic and climatic forcings into records of sediment supply and prove-
    nance, Scientific Reports, 9, 4115, https://doi.org/10.1038/s41598-019-39754-6, https://doi.org/10.1038/s41598-019-39754-6, 2019.

Shobe, C. M., Tucker, G. E., and Barnhart, K. R.: The SPACE 1.0 model: a Landlab component for 2-D calculation of sediment transport,
    bedrock erosion, and landscape evolution, Geoscientific Model Development, 10, 4577–4604, https://doi.org/10.5194/gmd-10-4577-2017,
760   https://gmd.copernicus.org/articles/10/4577/2017/, publisher: Copernicus GmbH, 2017.

Sklar, D. W.: Sediment and rock strength controls on river incision into bedrock, Geology, 29, 1087–1090, https://doi.org/10.1130/0091-7613(2001)029<1087:SARSCO>2.0.CO, 2001.

Sklar, L. and Dietrich, W.: River longitudinal profiles and bedrock incision models: Stream power and the influence of sediment supply, Rivers over rock: fluvial processes in bedrock channels, pp. 237–260, https://doi.org/10.1029/GM107p0237, 1998.

765   Sklar, L. S. and Dietrich, W. E.: Sediment and rock strength controls on river incision into bedrock, Geology, 29, 1087–1090, 2001.

Sklar, L. S. and Dietrich, W. E.: A mechanistic model for river incision into bedrock by saltating bed load, Water Resources Research, 40, 1–21, 2004.

Struth, L., García-Castellanos, D., Rodríguez-Rodríguez, L., Viaplana-Muzas, M., Vergés, J., and Jiménez-Díaz, A.: Topographic, lithospheric and lithologic controls on the transient landscape evolution after the opening of internally-drained basins. Modelling the North

770   Iberian Neogene drainage, BSGF - Earth Sciences Bulletin, 192, 45, https://doi.org/10.1051/bsgf/2021036, https://www.bsgf.fr/articles/bsgf/abs/2021/01/bsgf210013/bsgf210013.html, publisher: EDP Sciences, 2021.

Tarboton, D. G.: A new method for the determination of flow directions and upslope areas in grid digital elevation models, Tech. Rep. 2, https://doi.org/10.1029/96WR03137, publication Title: Water Resources Research Volume: 33, 1997.

Tofelde, S., Schildgen, T. F., Savi, S., Pingel, H., Wickert, A. D., Bookhagen, B., Wittmann, H., Alonso, R. N., Cottle, J., and Strecker, M. R.:

775   100 kyr fluvial cut-and-fill terrace cycles since the Middle Pleistocene in the southern Central Andes, NW Argentina, Earth and Planetary Science Letters, 473, 141–153, 2017.

Tofelde, S., Bernhardt, A., Guerit, L., and Romans, B. W.: Times Associated With Source-to-Sink Propagation of Environmental Signals During Landscape Transience, Frontiers in Earth Science, 9, https://www.frontiersin.org/article/10.3389/feart.2021.628315, 2021.

Tucker, G. E. and Bradley, D. N.: Trouble with diffusion: Reassessing hillslope erosion laws with a particle-based model, Journal of Geo-

780   physical Research: Earth Surface, 115, https://doi.org/10.1029/2009JF001264, https://agupubs.onlinelibrary.wiley.com/doi/abs/10.1029/2009JF001264, _eprint: https://agupubs.onlinelibrary.wiley.com/doi/pdf/10.1029/2009JF001264, 2010.

Tucker, G. E. and Slingerland, R.: Predicting sediment flux from fold and thrust belts, Basin Research, 8, 329–349, https://doi.org/10.1046/j.1365-2117.1996.00238.x, publisher: Blackwell Science Ltd., 1996.

Tucker, G. E., Hobley, D. E. J., Hutton, E., Gasparini, N. M., Istanbulluoglu, E., Adams, J. M., and Nudurupati, S. S.: CellLab-

785   CTS 2015: continuous-time stochastic cellular automaton modeling using Landlab, Geoscientific Model Development, 9, 823–839, https://doi.org/10.5194/gmd-9-823-2016, https://gmd.copernicus.org/articles/9/823/2016/, publisher: Copernicus GmbH, 2016.

von Neumann, J.: The general and logical theory of automata, in: Cerebral mechanisms in behavior; the Hixon Symposium, pp. 1–41, Wiley, Oxford, England, 1951.

Wang, L. and Liu, H.: An efficient method for identifying and filling surface depressions in digital elevation models for hydrologic analysis

790   and modelling, International Journal of Geographical Information Science, 20, 193–213, https://doi.org/10.1080/13658810500433453, publisher: Taylor & Francis, 2006.

Whipple, K. X., DiBiase, R. A., and Crosby, B. T.: Bedrock Rivers, in: Treatise on Geomorphology, vol. 9, pp. 550–573, Fluvial Geomorphology, https://doi.org/10.1016/B978-0-12-374739-6.00254-2, 2013.

Wolfram, S.: Cellular automata as models of complexity, Nature, 311, 419–424, https://doi.org/10.1038/311419a0, https://www.nature.com/

795   articles/311419a0, bandiera_abtest: a Cg_type: Nature Research Journals Number: 5985 Primary_atype: Reviews Publisher: Nature Publishing Group, 1984.

Yuan, X. P., Braun, J., Guerit, L., Rouby, D., and Cordonnier, G.: A New Efficient Method to Solve the Stream Power Law Model Taking Into Account Sediment Deposition, Journal of Geophysical Research: Earth Surface, https://doi.org/10.1029/2018JF004867, publisher: Wiley Online Library, 2019.